Investigation of the Curing Behavior of a Novel Epoxy Photo-Dielectric Dry Film (ViaLux™ 81) for High Density Interconnect Applications

RAJIV C. DUNNE,[1] SURESH K. SITARAMAN,[1] SHIJIAN LUO,[2] YANG RAO,[2] C. P. WONG,[2] WILLIAM E. ESTES,[3] CEFERINO G. GONZALEZ,[3] JOHN C. COBURN,[3] MOOKAN PERIYASAMY[3]

[1] The George W. Woodruff School of Mechanical Engineering, Georgia Institute of Technology, Atlanta, Georgia 30332

[2] School of Material Science & Engineering, Georgia Institute of Technology, Atlanta, Georgia 30332

[3] DuPont Photopolymers and Electronic Materials, Research Triangle Park, North Carolina 27709

Received 7 September 1999; accepted 30 January 2000

ABSTRACT: The objective of this work was to determine the cure kinetics of ViaLux™ 81 photo-dielectric dry film and to optimize its curing schedule for the fabrication of sequentially built up high density interconnect-printed wiring boards. Photosensitive epoxy materials such as the photo-dielectric dry film studied herein have complicated curing regimes. This is attributed to the long lifetime of the curing catalyst that is generated by ultraviolet exposure. Dynamic differential scanning calorimetry (DSC) experiments revealed a two-peak curing mechanism, which could not be separated at lower heating rates. The activation energies for the two cure events, calculated using the Kissinger method, were found to be 129 and 124 kJ/mol, respectively. A cure-dependent activation energy was also determined using the isoconversional method, and a "model-free" approach was adopted to simulate the evolution of degree-of-cure under dynamic and isothermal conditions. The results suggest that cure cycles of approximately 15 min at temperatures above 165°C can result in a degree-of-cure of 90% and above. This implies that faster fabrication is possible with either rapid thermal curing equipment or continuous cure surface mount technology furnaces. © 2000 John Wiley & Sons, Inc. J Appl Polym Sci 78: 430–437, 2000

Key words: high density interconnect-printed wiring boards (HDI-PWB); photo-dielectric dry film (PDDF); differential scanning calorimetry (DSC); cure kinetics; isoconversional method

INTRODUCTION

The high density interconnect–printed wiring boards (HDI–PWB) is a fast-evolving, cost-competitive technology because of its proven capabilities of mounting high I/O chips and supporting high wiring density. In typical HDI thin film processing using photo-dielectric dry films (PDDFs), the photosensitive dielectric material is first laminated onto an FR4 epoxy-glass laminate board and then ultraviolet (UV) exposed and post-exposure baked to define the interconnect vias (microvias) and conductor line patterns. Then, the PDDF is developed in an appropriate solvent, and thermally baked to complete the curing of the

Correspondence to: S. Sitaraman (suresh.sitaraman@me.gatech.edu).

Contract grant sponsor: National Science Foundation; contract grant number: CAREER-DMI-9702285.

Contract grant sponsor: Packaging Research Center; contract grant number: EEC-9402723.

Journal of Applied Polymer Science, Vol. 78, 430–437 (2000)
© 2000 John Wiley & Sons, Inc.

film. An additive or subtractive electroless and/or electrolytic plating process is used for metallization of the vias and lines.[1–3] After metallization, the next layer of PDDF is laminated, exposed, post-exposure baked, developed and cured, and the metallization process is repeated. This sequential alternate layering of dielectric and metallization creates the multi-layered HDI substrate. The dry film format is advantageous because it allows a wide range of thicknesses, tighter thickness control, high degree of planarity, and a solvent-free coating free of pinhole defects. It is important to understand the cure kinetics of the interlayer PDDF material to ensure the accuracy and registration of the fine interconnect features as well as the thermomechanical integrity of the finished multi-layered structure.

In this work, an uncured, A-stage epoxy-based photo-imageable dielectric dry film called ViaLux™ 81 is considered. The UV exposure process first induces the photolytic decomposition of the cationic photoinitiator to create a superacid. When heated further, the superacid promotes sufficient crosslinking for the microvia image to be defined. The photoinitiator typically has a long lifetime in the system and is responsible for assisting additional thermal crosslinking. Such cationic photo-epoxies are examples of so-called "living polymerizations," and their influence cannot be ignored in cure kinetics and in practical processing schemes.[4–6]

An understanding of the degree-of-cure (DOC) evolution in ViaLux™ 81 is useful because this knowledge can be used to aid circuit designs, to widen processing latitudes, to estimate the effects of thermal events in sequentially built up layers, and to control the stresses from component assembly/rework or thermal shock testing.[7] In addition, emerging Plastic Ball Grid Array packages and HDI-PWBs will be operating in the range of 1–5 GHz.[8] The electrical properties, especially the dielectric loss, can be dramatically increased by characteristic resonances of poorly cured oligomers, by dielectric absorption of polarization from bond breakage during decomposition, and by losses due to segmental motion of open bonds that can arise from either a low DOC or the onset of thermal decomposition.[9]

The objective of this work was to determine the curing kinetics of the Vialux™ 81 (PDDF) with the aim of understanding and optimizing the curing schedule. Initial dynamic differential scanning calorimetry (DSC) scans at 5–10°C/min revealed a two-peak curing mechanism, which could not be separated at lower heating rates. On the other hand, the initial exotherm from DSC isothermal experiments showed a rapid reaction rate at the beginning with only a single peak. Significant heat flow losses could occur at the start when the sample is trying to equilibrate at the prescribed isothermal temperature, as well as near the apparent completion of the reaction when the reaction rate falls below the sensitivity of the calorimeter. Therefore, the faster multiple heating rate experiments were conducted to capture the complexity of the curing reaction, and to determine the time–temperature dependence of conversion, i.e., $\alpha = f(t,T)$. This method is very useful for material systems that have multiple reactions, unresolved baselines, or residual solvents.[10] The lack of material composition information makes the kinetic analysis presented herein strictly phenomenological in nature. However, such an analysis can yield a "processing window" for a wide range of potential applications, and allows one to obtain a consistent product with the desired physical and mechanical properties.

EXPERIMENTAL

ViaLux™ 81 PDDFs of 75-μ thickness were used in this work. As supplied, the PDDF is sandwiched between two protective sheets: a polyethylene film that is removed before lamination and a Mylar cover sheet that is removed before post-exposure bake. Free standing films for the DSC experiments were prepared by laminating the PDDF onto a Teflon sheet using a DuPont VACREL® laminator (SMVL-100) at 70°C and 4 bar pressure for 1 min. UV exposure was done in a Tamarack Scientific™ exposure tool.

To determine the weight loss characteristics, the TA Instruments 2050 Thermo Gravimetric Analyzer™ (TGA) was used. A single scan at 5°C/min was done from room temperature to 500°C on a 16.5 mg sample. DSC measurements were performed in a TA Instruments 2920 MDSC™ (modulated differential scanning calorimetry) instrument. Both dynamic heating rate and isothermal experiments were performed. Because of the presence of some solvents in the material, smaller sample sizes of 5–8 mg were used in hermetically sealed aluminum pans and in a nitrogen purge gas environment. Care was taken to minimize and to standardize the time between exposure and subsequent DSC analysis. The dynamic heat-

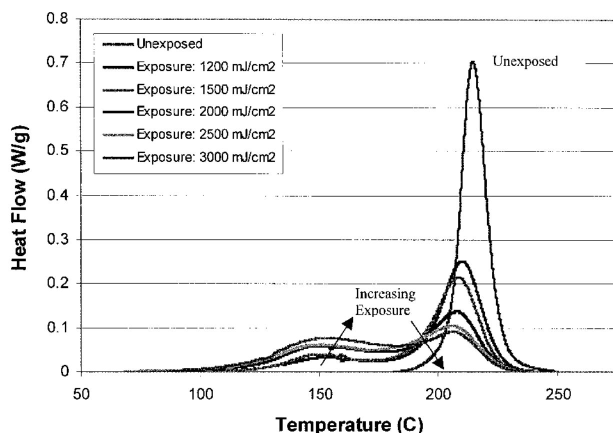

Figure 1 Effect of varying UV exposure on uncured samples.

ing rate experiments were conducted from room temperature to 350°C at six different heating rates: 2, 3, 5, 10, 15, and 20°C/min. A subsequent dynamic scan at 10°C/min was done to confirm that the sample had cured completely, and to determine the glass transition temperature (T_g). These experiments were repeated three times to establish the reproducibility of the results. The isothermal experiments were done from 110 to 175°C in 5°C increments for a duration of 60 min. A subsequent dynamic scan was done at 10°C/min on each of these samples to determine the residual heat of reaction, if any.

RESULTS AND DISCUSSION

Effect of Varying Exposure

As mentioned above, exposure is required for photo imaging the via and circuit patterns. Consistent with that, uncured samples were exposed to different exposure doses (1200, 1500, 2000, 2500, and 3000 mJ/cm^2) to study the effect of exposure on curing. Results from a dynamic DSC scan at 5°C/min from room temperature to 300°C on each of these samples are shown in Figure 1. The unexposed sample shows a single peak at 215°C, whereas the samples irradiated with UV light (λ = 365 nm, irradiance = 7.8 mW/cm^2) show two curing peaks. The cationic photoinitiator present in the film creates superacid (H^+) because of photolytic decomposition when the film is exposed to UV light. The H^+ initiates the ring opening polymerization of epoxy group. The propagation of epoxy polymerization takes place partially at lower temperatures (first DSC peak at 154°C) and polymerization continues with higher conversion of epoxy to polymer when the temperature is increased (second peak in the DSC at 210 ± 2°C). However, when there is no UV exposure, the photoinitiator thermally decomposes and creates superacid (H^+) when the temperature is above 180°C, and this superacid initiates and propagates the epoxy polymerization. Therefore, the unexposed sample exhibits only one DSC peak.

With an increase in the exposure dose, the area under the first peak increases whereas the area under the second peak decreases. This indicates that more curing takes place around the lower temperature peak as the exposure dose is increased. This is because of the increase in the concentration of the superacid generated with the increase in exposure dose. However, beyond an exposure dose of 2000 mJ/cm^2, the gain in terms of the DOC achieved at the end of the first reaction is minimal compared with the increase in exposure time. Therefore, in all subsequent experiments, the samples were exposed to 2000 mJ/cm^2. This is beneficial from the HDI board processing and reliability standpoint because one would prefer to select a lower processing temperature to cure the material. The increase in the exposure time is more than offset by the significant reduction in the postexposure enhancement bake and final thermal bake time of the dielectric, as shown in later sections. However, in selecting an optimum curing schedule, one should take note of the fact that at low exposure doses, the PDDF might be insufficiently crosslinked at the bottom of the film, and swelling or liftoff of the film will result during the development process, whereas at excessive exposure doses, the via resolution will deteriorate because of light scattering off the underlying surfaces.

Thermogravimetric Analysis

In Figure 2, the weight loss characteristics of the uncured ViaLux™ 81 PDDF are shown. The initial weight loss is small, and occurs around 55°C because of the presence of a low boiling solvent. The additional weight loss observed around 145°C is due to a high boiling solvent, and is about 5%. The material seems to be thermally stable for temperatures up to approximately 320°C.

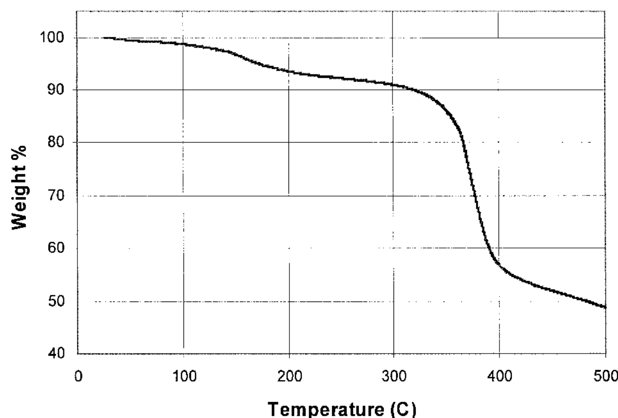

Figure 2 Thermogravimetric curve of ViaLux™ 81 PDDF.

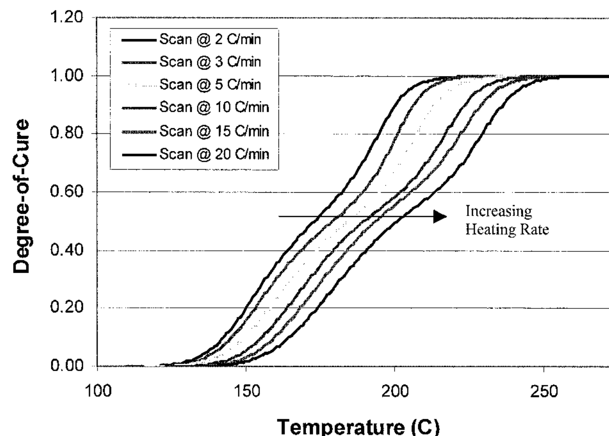

Figure 4 Evolution of DOC with temperature.

Dynamic DSC

The results from the multiple heating rate experiments illustrated in Figure 3 reveal two curing peaks. The peak temperatures shift predictably to higher temperatures with an increase in the heating rate, as more heat flow is required to cure the material at a faster heating rate.

The total enthalpy of the curing reaction or the ultimate heat of reaction, H_{ult}, is computed from the total area under each heating rate curve divided by the respective heating rate value. If one assumes that the DOC (α) is proportional to the heat generated during the reaction, that is, $\alpha = H/H_{ult}$, the DOC at the peaks and the valley as well as the evolution of DOC with temperature can be calculated. The change in the curing reaction mechanism as the curing proceeds at the higher temperatures is clearly evident from the change in slope in the evolution of DOC with temperature in Figure 4.

In addition, from Table I, the ultimate heat of reaction, H_{ult}, as well as the DOC at the peak temperatures and the valley, are almost independent of the heating rate. The less than 5% inconsistency in H_{ult} may be attributed to the use of a linear baseline correction, as well as to the sensitivity of the experimental results to sample sizes and environmental conditions such as light and moisture. No residual exotherm was observed in the subsequent dynamic scan done at 10°C/min from room temperature to 300°C. This implied that the material was fully cured. The T_g, determined from the midpoint in the step change in the heat flow data, was at 99.15°C.

Isothermal DSC

The heat flow exotherms from the isothermal experiments and the subsequent dynamic scan at

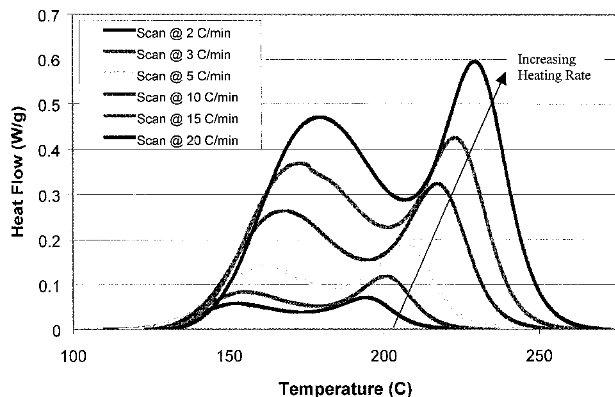

Figure 3 Dynamic DSC data (baseline corrected) at multiple heating rates (exposure = 2000 mJ/cm^2).

Table I Calculation of Ultimate Heat of Reaction and DOC at the Peaks and Valley

Heating Rate, β (°C/min)	H_{ult} (J/g)	DOC at 1st Peak	DOC at 2nd Peak	DOC at Valley
2	111.19	0.24	0.80	0.51
3	117.44	0.22	0.79	0.49
5	123.27	0.24	0.80	0.50
10	116.95	0.26	0.80	0.54
15	111.04	0.26	0.81	0.57
20	112.84	0.26	0.80	0.55
Average values	115.46	0.25	0.80	0.53

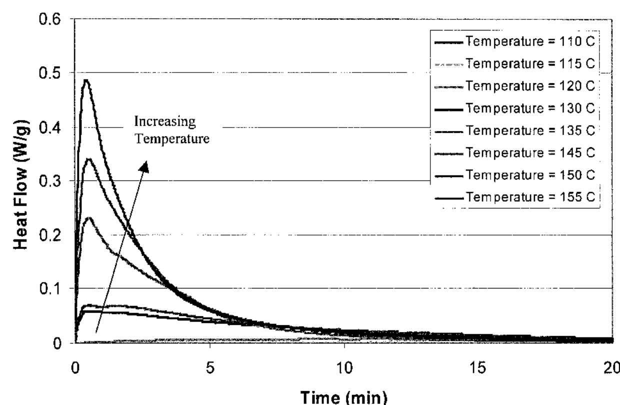

(a)

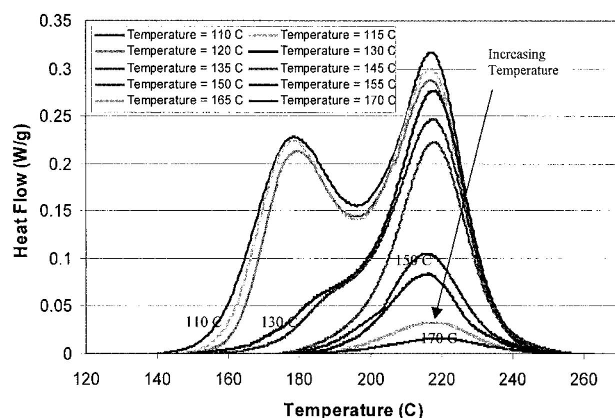

(b)

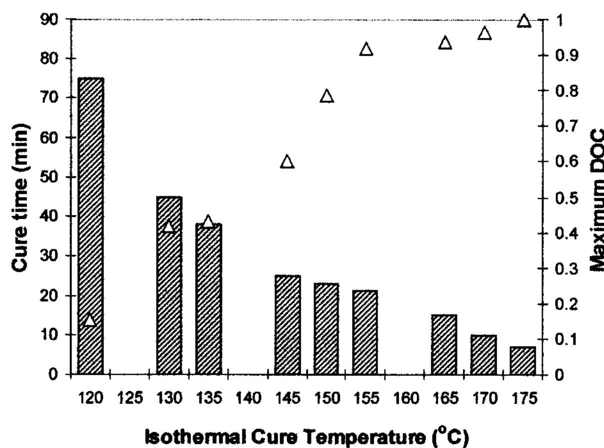

Figure 5 (a) Isothermal DSC data (baseline corrected) at different temperatures (exposure = 2000 mJ/cm^2) (abscissa scaled for clarity). (b) Subsequent DSC scan data (baseline corrected) of the isothermally cured samples (exposure = 2000 mJ/cm^2). (c) Maximum DOC and cure times at the different isothermal temperatures (vertical bars denote cure time; filled triangles denote maximum DOC).

10°C/min are shown in Figure 5(a) and (b), respectively. From the dynamic scans, it is evident that curing is incomplete at all of these temperatures. No residual exotherm is observed however when the cure temperature is increased to 175°C, indicating complete cure of the material at this temperature. The heat of reaction at each of the isothermal temperatures, ΔH_T, as well as the residual heat, ΔH_{res}, from the subsequent dynamic scan are calculated from the area under the curves. The addition of ΔH_T and ΔH_{res} yields the ultimate heat of reaction, H_{ult}. The T_g, calculated from the midpoint in the step transition of the completely cured samples, was at 102 ± 2°C. This T_g is consistent with that obtained from dynamic DSC experiments.

As seen in Figure 5(b), when isothermal curing is done at or above 145°C, the first reaction is complete, and the DSC scan reveals an exotherm only for the second peak reaction. The total isothermal curing time at this temperature is less than 30 min. The maximum DOC at each of the isothermal cure temperatures along with the curing time is illustrated in Figure 5(c). A rapid increase in the maximum DOC at 145°C is accompanied with a simultaneous reduction in the isothermal curing time. At 165°C, the cure duration is approximately 15 min and the DOC is about 93%. Full cure is achieved at a cure temperature of 175°C, with the cure duration being less than 10 min. However, it is important to emphasize that in sequential HDI processing, 100% cure of the dielectric is not always desirable, because its adhesion to the subsequent metal and dielectric layers will deteriorate with higher DOC.[11]

CURE-KINETICS MODELING

The primary objective of this work was to develop a predictive cure kinetics model for the evolution of DOC with time and temperature under any arbitrary temperature-time curing profile, using the experimental data from multiple heating rate DSC experiments.

Theory

The basic rate equation which expresses the reaction rate as a function of time or temperature with conversion is:

$$\frac{d\alpha}{dt} = k(T)f(\alpha) = Ae^{-E/RT}f(\alpha) \tag{1}$$

where, α is the DOC, $f(\alpha)$ is the reaction model, k is the rate constant, A is the pre-exponential or frequency factor, E is the activation energy, R is the gas constant, T is the temperature, and t is the time. Under nonisothermal conditions, when the temperature varies with time at a constant heating rate, $\beta = dT/dt$, this equation may be transformed as:

$$\frac{d\alpha}{dt} = \frac{d\alpha}{dT}\frac{dT}{dt} = \frac{d\alpha}{dT}\beta = Ae^{-E/RT}f(\alpha) \tag{2}$$

Equation (2) is often expressed in an integral form as:

$$\int_0^\alpha \frac{d\alpha}{f(\alpha)} = g(\alpha) = \frac{A}{\beta}\int_0^T e^{-E/RT}\,dT \tag{3}$$

Because a closed form solution for the temperature integral does not exist, a number of approximations have been suggested in the literature.[12–14] The two reaction models that are used most often for thermosetting systems are the nth order, where $f(\alpha) = (1 - \alpha)^n$, or autocatalytic models, where $f(\alpha) = \alpha^m(1 - \alpha)^n$.

Cure Kinetics Model

Equation (1) is typically used for single peak reactions. However, it can be used for multiple peak reactions as well.[15,16] To determine the kinetic model, one needs to evaluate the kinetic triplet: activation energy (E), frequency factor (A), and the reaction order.

Two different approaches have been used to compute the activation energy from the dynamic scan data at multiple heating rates. In the Kissinger method, only peak temperature (T_p) information is required to compute the activation energy corresponding to the two peak reactions.[17] As shown in Figure 6, $\ln(\beta/T_p^2)$ is plotted versus $1/T$ for the six heating rate dynamic scan experiments. Using linear regression, the slope of the data (E/R) corresponding to the two peaks is evaluated. The activation energy corresponding to the first and second peaks is 129.17 kJ/mol and 124.24 kJ/mol, respectively. This method is advantageous for cases in which there are solvent effects and unresolved baselines, as is in this work.

An alternate approach to calculate the activation energy is the Isoconversional method, which

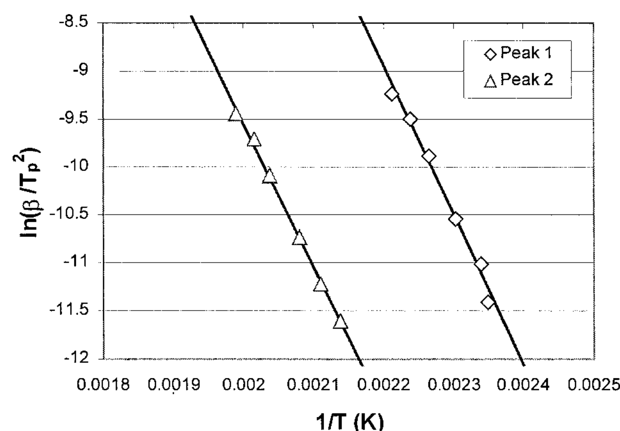

Figure 6 Calculation of activation energy (Kissinger's method).

is based on the principle that the reaction rate at a particular conversion is dependent only on temperature. A cure-dependent activation energy, E_α, is calculated from the logarithmic form of the rate equation using Friedman's method[11,18,19]:

$$\ln(d\alpha/dt)_{\alpha,i} = \ln[Af(\alpha)]_{\alpha,i} - E_\alpha/RT_{\alpha,i} \tag{4}$$

where the subscript α refers to the value related to a particular conversion, and i to a given heating rate. The activation energy at each DOC is calculated using linear regression, from a plot of $\ln(d\alpha/dt)$ versus $1/T$ at that DOC for the six heating rate dynamic scan experiments [see Fig. 7(a)]. One can see the complex dependence of the activation energy with the DOC in Figure 7(b). Averaging of such systematic dependencies of activation energy on DOC should be avoided, because the complexity of the process will then not be captured.[20,21]

However, estimation of the two remaining kinetic parameters, frequency factor (A) and order of reaction is difficult. This is due to the lack of information about the reaction mechanisms, the variation of the activation energy with DOC, and the inability to deconvolute of the reaction peaks.

To circumvent these problems, a "model-free" approach suggested by Vyazovkin[20] has been used in this study. In this approach, it is assumed that the partial kinetic triplets, related to a given conversion, do not change with temperature. Using this assumption, one can calculate the DOC evolution at any arbitrary isothermal temperature (T_o) or heating rate (β_o) by using the 4th order Runge Kutta method to solve eqs. (5) and (6) respectively, with knowledge about the α-T de-

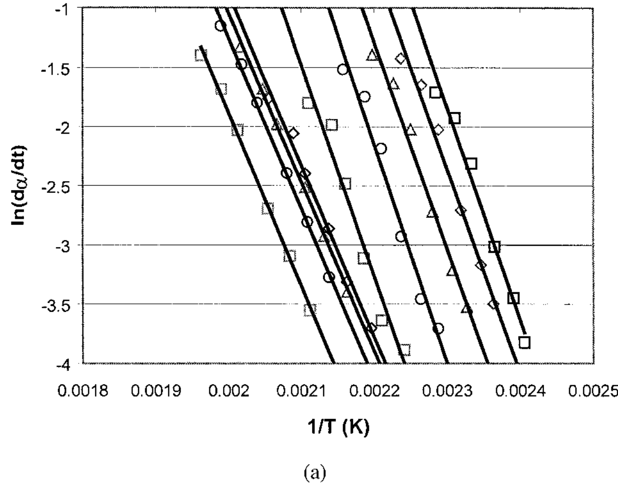

(a)

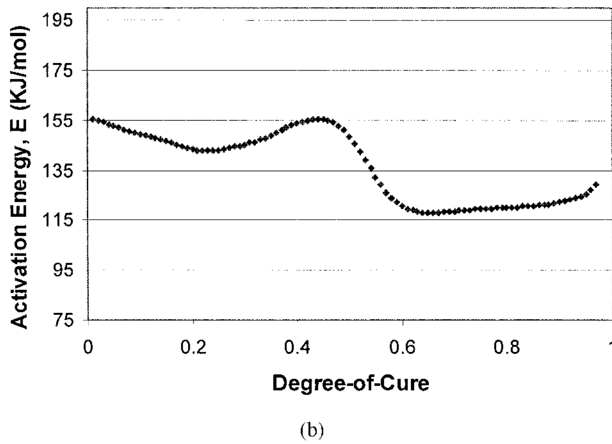

(b)

Figure 7 (a) Calculation of cure-dependent activation energy (isoconversional method). (b) Activation energy versus DOC.

pendence from any single experimental heating rate (β) data:

$$t_{\alpha}^{\text{calculated}} = [\beta \exp(-E_{\alpha}/RT_o)]^{-1} \int_0^{T_\alpha} \exp(-E_\alpha/RT)\, dT \quad (5)$$

$$(1/\beta) \int_0^{T_\alpha} \exp(-E_\alpha/RT)\, dT = (1/\beta_o) \int_0^{T_\alpha^{\text{calculated}}} \exp(-E_\alpha/RT)\, dT \quad (6)$$

It should be mentioned that these equations do not incorporate both the kinetic model and the frequency factor. If the kinetic triplets do not change with temperature, the frequency factor and the order of reaction are not necessary in extrapolating experimental results to other sets of conditions. Additionally, the dependence of E_α on α in the above equations takes into account the total complexity of the process.

Figure 8(a) shows the comparisons between the DOC evolution from the dynamic DSC experimental data as shown in Figure 4 and the theoretical calculations as given by eq. (6). The theoretical calculations were done for β_o = 3, 5, 10, 15, and 20°C/min using the β = 2°C/min experimental DSC data as the reference. Excellent agreement is observed through the entire range of curing. However, from Figure 8(b), it can be observed that this method is inadequate to predict the DOC evolution under isothermal conditions. The iso-

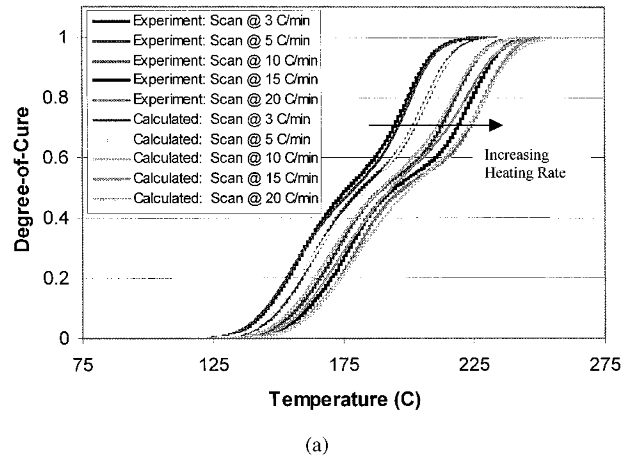

(a)

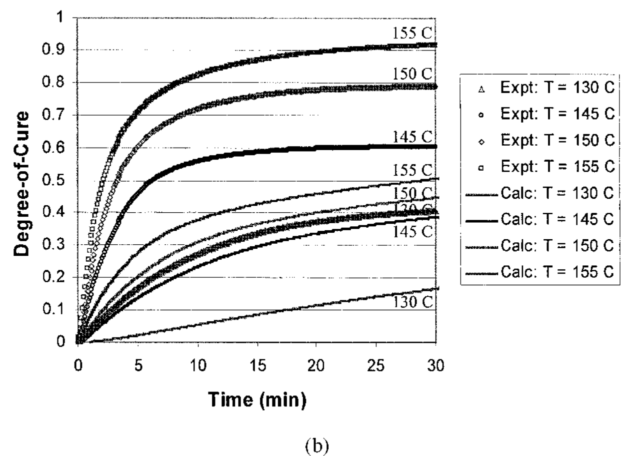

(b)

Figure 8 (a) Comparison of experimental and calculated DOC evolution with temperature (for dynamic DSC data). (b) Comparison of experimental and calculated DOC evolution with time (for isothermal DSC data).

thermal theoretical calculations were done for T_o = 130, 145, 150, and 155°C using eq. (5) with the β = 2°C/min experimental DSC data as the reference.

Alternate models based on deconvolution of the peak reactions in the dynamic DSC data are presently being developed, and will be reported in a future publication. In addition, a cure kinetics model based on isothermal DSC data will also be developed, which will facilitate optimization of the Vialux™ 81 cure processing parameters.

CONCLUSIONS

We have shown that the curing mechanism for ViaLux™ 81 PDDF is complex, but amenable to a detailed analysis. The determination of the kinetic triplets proved to be difficult because of multiple peak reactions. A "model-free" approach using a cure-dependent activation energy seems to produce good results for the DOC evolution under heating rate conditions, but performs poorly under isothermal conditions. The isothermal DSC experiments suggest that high degrees of cure can be achieved within approximately 15 min when the cure temperature is above 165°C.

This work has important implications in HDI substrate fabrication:

1. Increasing the UV exposure dose up to 2000 mJ/cm^2 allows much faster thermal curing cycles.
2. Rapid thermal curing of ViaLux™ 81 on silicon wafers should be possible in Wafer Level-Chip Scale Packages.
3. Fast cure cycles suggest that HDI-PWBs could possibly be cured in continuous belt furnaces that are similar to SMT reflow equipment.

Future work will involve the comprehensive thermal and mechanical characterization of the Vialux™ 81 system. This will include the determination of the heat capacity, thermal conductivity, cure-dependent stress relaxation modulus, and the thermal expansion coefficient of the PDDF material, as well as a cure shrinkage study.

The authors thank Professor J. V. Crivello (Department of Chemistry, Rensselaer Polytechnic Institute) for the helpful discussions concerning the chemistry of cationic initiators. Also, the authors acknowledge the support from the National Science Foundation and the Packaging Research Center.

REFERENCES

1. Dunne, R. C.; Sitaraman, S. Proc 48th Electron Compon Technol Conf; IEEE: Piscataway, NJ, 1998, pp. 353–361.
2. Gonzalez, C. G.; Estes, W. E.; Raman, S. Presented at the Electronic Circuits World Conference 8, Tokyo, Japan, 1999. See also ViaLux™ 81 Process Data Sheets, DuPont.
3. Coombs, C. F. Printed Circuits Handbook; McGraw-Hill: New York, 1988.
4. Crivello, J. V.; Dietliker, K. In Speciality Finishes: Chemistry and Technology of UV and EB Formulations for Coatings, Inks, and Paints; Oldring, P. K. T., Ed.; John Wiley & Sons: New York, 1998.
5. Crivello, J. V. In UV Curing: Science and Technology; Pappas, S. P., Ed.; Technology Marketing Corporation: Connecticut, 1978.
6. Russel, D. J. Presented at the IPC Printed Circuits Exposition, Long Beach, CA, 1998, Paper S17–5-1.
7. Alvino, W. M. In Plastics for Electronics: Materials, Properties and Design Specifications; McGraw-Hill: New York, 1995; Chapters 2–4.
8. Estes, W. E.; Gonzalez, C. G.; Overcash, T. R.; Murray, E. B.; Coburn, J. C.; Periyasamy, M.; Reckert, T.; Smith, R. L.; Muenzel, N. Presented at the IPC Chip Scale and BGA Symposium, Santa Clara, CA, 1999.
9. Ku, C. C. Liepens, R. In Electrical Properties of Polymers: Chemical Principles; Hanser Publishers: Munich, 1987; Chapters 2, 3.
10. Prime, R. B. In Thermal Characterization of Polymer Materials, 2nd ed.; Turi, E. A., Ed.; Academic Press: San Diego, 1997; Chapter 6.
11. Strandjord, A. J. G.; Scheck, D. M.; Rogers, W. B.; Garrou, P. E.; Ida, Y.; Cummings, S. L. Int J Microcircuits Electron Packag 1996, 19, 260–280.
12. Flynn, J. H. J Therm Anal 1983, 27, 95.
13. Quanyin, R.; Su, Y. J Therm Anal 1995, 44, 1147.
14. Ortega, A.; Perez–Maqueda, L. A.; Criado, J. M. Thermochim Acta 1996, 282, 29.
15. Barton, J. M. Adv Polym Sci 1985, 72, 111–154.
16. Duswalt, A. A. Thermochim Acta 1974, 8, 57.
17. Montserrat, S.; Flaque, C.; Pages, P.; Malek, J. J Appl Polym Sci 1995, 56, 1413.
18. Flynn, J. H. J Therm Anal 1991, 37, 293.
19. Montserrat, S.; Malek, J. Thermochim Acta 1993, 228, 47.
20. Vyazovkin, S. Int J Chem Kinet 1995, 28, 95.
21. Vyazovkin, S.; Wright, C. A. J Phys Chem 1997, 101, 8279.